Center for Turbulence Research
Proceedings of the Summer Program 1994

On the asymptotic similarity of rotating homogeneous turbulence

By K. D. Squires[1], J. R. Chasnov[2] AND N. N. Mansour[3]

Asymptotic similarity states at large Reynolds numbers and small Rossby numbers in rotating homogeneous turbulence are investigated using the database obtained from large-eddy simulations of the incompressible Navier-Stokes equations. Previous work has shown that the turbulence kinetic energy and integral length scales are accurately described by simple scaling laws based on the low wavenumber part of the three-dimensional energy spectrum (Squires *et al.* 1994). The primary interest of the present study is to search for spectrum similarity in the asymptotic state. Four independent energy spectra are defined. It is shown that rescaling of these energy spectra in the asymptotic regime will collapse three out of the four spectra. The spectrum which does not collapse is a function only of the vertical wavenumber and corresponds to two-component motions in the plane normal to the rotation axis. Detailed investigation of the cause of this anomalous behavior reveals the existence of a strong reverse cascade of energy from small-to-large scales of the two-dimensional, two-component motions. This feature of the rotating flow is presumably linked to the lack of a complete similarity state, though further study of this issue is required.

1. Introduction

Solid-body rotation of initially isotropic turbulence represents the most basic turbulent flow whose structure is altered by system rotation but without the complicating effects introduced by mean strains or flow inhomogeneities. Squires, Chasnov, Mansour & Cambon (1994) (referred to as SCMC throughout this manuscript) examined the long-time, asymptotic evolution of rotating homogeneous turbulence at large Reynolds numbers and small Rossby numbers. They found that the kinetic energy decay exponent was reduced by approximately a factor of two relative to its value in non-rotating turbulence and was independent of the rotation rate. SCMC also found that the integral length scales undergo power-law growth and that the evolution of both the kinetic energy and length scales in the asymptotic regime is accurately described using simple scaling laws based on the invariants of the low wavenumber part of the initial energy spectrum.

1 The University of Vermont
2 The Hong Kong University of Science and Technology
3 NASA Ames Research Center

The scaling laws of the kinetic energy and integral length scales deduced by SCMC suggest the existence of an asymptotic similarity state in rotating homogeneous turbulence. Since a similarity state permits prediction of the flow evolution using a simple rescaling of the statistics, existence of asymptotic similarity states enables prediction of the ultimate statistical evolution of the flow without detailed knowledge of non-linear transfer processes. Similarity states thus imply a certain universal character to a flow which may ultimately simplify modeling of complex turbulent flows at high Reynolds numbers.

The objective of the present work, therefore, is to search an asymptotic similarity state for the energy spectra. In §2 an overview of the LES database used in this study is summarized. Also presented in §2 is the time development of the kinetic energy power-law exponent, integral length scales, and asymptotic scaling laws obtained from both dimensional analysis and the simulation database. The reader is referred to Squires *et al.* (1993, 1994) for a more complete discussion. In §3 the asymptotic spectrum similarity is analyzed and tested using the LES database.

2. Database overview and scaling laws

2.1 Database overview

The database used in the present study was obtained using large-eddy simulation of the incompressible Navier-Stokes equations in a rotating frame of reference. The use of a large-eddy simulation with zero molecular viscosity ensures that the flows considered are nominally at infinite Reynolds numbers. For purposes of discussion the vertical (x_3) axis is taken along the axis of rotation. The governing equations were solved using the pseudo-spectral method developed by Rogallo (1981). Subgrid-scale motions were parameterized using a spectral-eddy viscosity modified for system rotation (Kraichnan 1976, Chollet & Lesieur 1981, Aupoix 1984). Calculations were performed from isotropic Gaussian initial conditions using an initial energy spectrum of the form

$$E(k,0) = \frac{1}{2} C_s \frac{u_0^2}{k_p} \left(\frac{k}{k_p}\right)^s \exp\left[-\frac{1}{2} s \left(\frac{k}{k_p}\right)^2\right], \tag{1}$$

where C_s is given by

$$C_s = \sqrt{\frac{2}{\pi}} \frac{s^{\frac{1}{2}(s+1)}}{1 \cdot 3 \cdot \ldots \cdot (s-1)} \tag{2}$$

and k_p is the wavenumber at which the initial energy spectrum is maximum. SCMC performed simulations with $s = 2$ and $s = 4$, corresponding to the initial energy spectrum having a low wavenumber form proportional to either k^2 or k^4.

Simulations were performed using resolutions of $128 \times 128 \times 512$ on a computational domain which is four times longer along the rotation axis than in the other directions. This yields an isotropic grip in physical space, but permits the development of large-scale anisotropies without compromising the usefulness of the computational results. The maximum wavenumber in each of the three coordinate

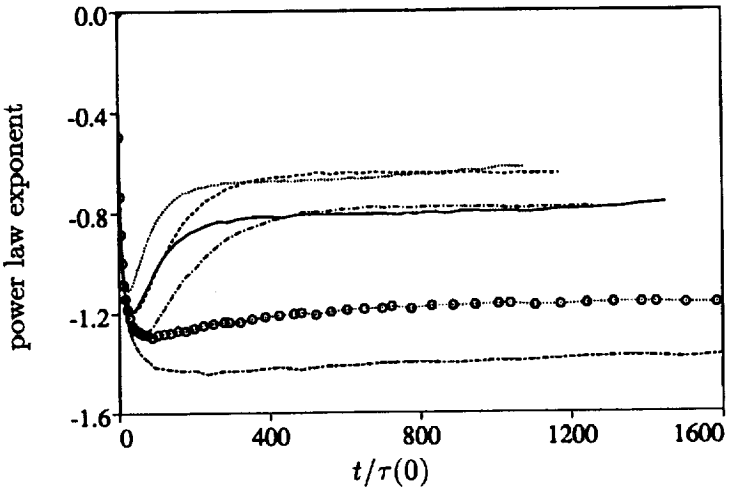

FIGURE 1. Time development of the power-law exponent of $\langle \mathbf{u}^2 \rangle$ in rotating turbulence. k^2 spectrum: o·····o $\Omega = 0$; ---- $\Omega = 0.5$; ····· $\Omega = 1.0$. k^4 spectrum: —— $\Omega = 0$; —·— $\Omega = 0.5$; —— $\Omega = 1.0$.

directions was 95, the initial root-mean-square velocity fluctuation u_0 was 1/2, and the wavenumber at which the initial spectrum was initially maximum, k_p, was 75. For each spectrum type, i.e., low wavenumber part proportional to k^2 or k^4, simulations results are available for three rotation rates, $\Omega = 0$, 0.5, and 1.0. The flows were evolved over a sufficiently long period so that the effects of rotation on the flow dynamics were clearly evident, and the kinetic energy decay and integral length-scale growth approximated power-law forms. This corresponds to an evolution of the flow to low Rossby numbers, where the Rossby number is a measure of the relative strength of inertial forces to Coriolis forces.

2.2 Statistical evolution and scaling laws

The effect of rotation on the evolution of the turbulence kinetic energy ($\langle \mathbf{u}^2 \rangle$) can be illustrated through examination of the power-law exponent, n (in $\langle \mathbf{u}^2 \rangle \propto t^{-n}$, see Fig. 1). In Fig. 1, the time axis is made dimensionless using the eddy turnover time in the initial field

$$\tau(0) = L_u(0)/\langle \mathbf{u}^2 \rangle^{1/2} \tag{3}$$

where $L_u(t)$ is the velocity integral scale at time t defined as

$$L_u(t) = \frac{\pi}{2} \frac{\int_0^\infty k^{-1} E(k,t) dk}{\int_0^\infty E(k,t) dk}. \tag{4}$$

Power-law exponents have been plotted for each initial spectrum type and rotation rate used in the calculations. It is evident from Fig. 1 that following an initial transient the power-law exponent becomes independent of time. Comparison of the power-law exponents for both initial spectrum types demonstrates the reduction

in the decay rate of kinetic energy in rotating turbulence. It is also clear from Fig. 1 that in the asymptotic regime the power-law exponent of the kinetic energy is independent of the rotation rate provided the rotation is non-zero. The value of the exponent depends only on the form of the initial energy spectrum.

It is possible to derive the appropriate asymptotic scalings of $\langle \mathbf{u}^2 \rangle$ for non-rotating turbulence using dimensional analysis (e.g., see Chasnov 1994). For the rotating flow, assuming that non-linear triadic interactions are correlated over a time scale directly proportional to Ω, SCMC showed that the asymptotic scalings for the kinetic energy are

$$\langle \mathbf{u}^2 \rangle \propto B_0^{\frac{2}{5}} t^{-\frac{6}{5}} (\Omega t)^{\frac{3}{5}} \quad (k^2 \text{ spectrum}) \tag{5}$$

$$\langle \mathbf{u}^2 \rangle \propto B_2^{\frac{2}{7}} t^{-\frac{10}{7}} (\Omega t)^{\frac{5}{7}} \quad (k^4 \text{ spectrum}). \tag{6}$$

For the k^2 spectrum B_0 is invariant while for the k^4 initial conditions B_2 is time dependent. However, the time dependence of B_2 is weak relative to the overall turbulence decay. It is assumed invariant for the purposes of developing asymptotic scalings. The scaling laws (5) and (6) predict that in rotating turbulence the kinetic energy decay exponent is reduced by a factor of two, relative to its value in the non-rotating flow. As shown by Fig. 1, simulation results agree with these predictions.

SCMC also examined the development of the integral length scales. These length scales are obtained from integration of the two-point correlation function

$$L_{\alpha\alpha;\beta} = \frac{1}{\langle u_\alpha^2 \rangle} \int \langle u_\alpha(\mathbf{x}) u_\alpha(\mathbf{x} + r\mathbf{e}_\beta) \rangle dr_\beta \,, \tag{7}$$

where $\mathbf{e}_\beta$ is the unit vector in the β direction, and α, $\beta = 1$, 2, or 3. The length scale $L_{\alpha\alpha;\beta}$ measures the correlation between the α velocity components with separation in the β direction. SCMC examined the evolution of five length scales. In the horizontal plane these integral scales are

$$L_{h1} = \frac{1}{2}(L_{11,1} + L_{22,2}), \quad L_{h2} = \frac{1}{2}(L_{11,2} + L_{22,1}), \quad L_{h3} = \frac{1}{2}(L_{33,1} + L_{33,2}). \tag{8}$$

The integral scale L_{h1} measures the horizontal correlation of longitudinal horizontal velocities, L_{h2} the horizontal correlation of lateral horizontal velocities, and L_{h3} the horizontal correlation of vertical velocities. For vertical correlations (along the axis of rotation) there are two independent integral scales

$$L_{v1} = \frac{1}{2}(L_{11,3} + L_{22,3}), \qquad L_{v2} = L_{33,3} \,, \tag{9}$$

where L_{v1} measures the vertical correlation of horizontal velocities and L_{v2} the vertical correlation of vertical velocities.

Shown in Fig. 2 is the time development of the integral scales from SCMC for the highest rotation rate used with each initial condition type. Also shown for reference is the slope corresponding to the asymptotic growth rate in non-rotating isotropic

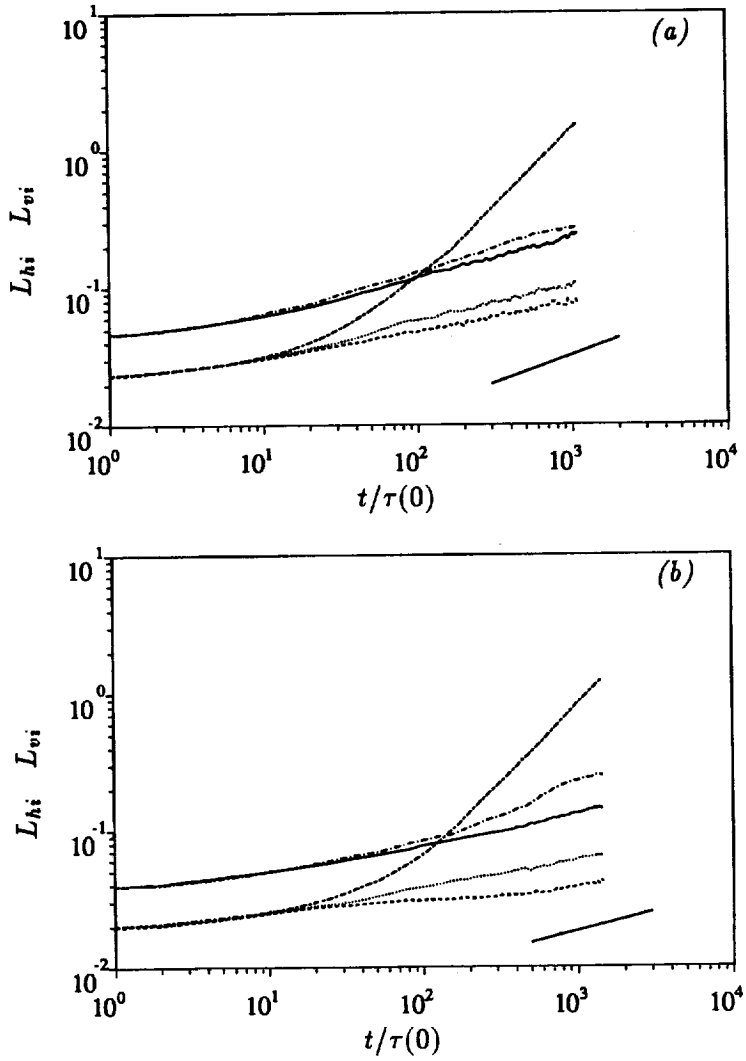

FIGURE 2. Time development of integral length scales in rotating turbulence, $\Omega = 1$. Asymptotic growth rate in non-rotating turbulence also shown in lower portion of figure. —— L_{h1}; ---- L_{h2}; ····· L_{h3}; —·— L_{v1}; —·— L_{v2}. (*a*) k^2 spectrum; (*b*) k^4 spectrum.

turbulence. It is clear from Fig. 2 that L_{v1} grows much more rapidly than all other integral scales. Also, the growth of the other four integral scales appear to be slightly suppressed relative to the non-rotating case. In addition, the simulations provide evidence that all the integral length scales exhibit power-law growth asymptotically and, with the important exception of L_{v1}, the power-law exponents are all the same. Thus, in the horizontal plane there appears to be a single independent length scale, which we denote generically as L_h, whereas there exists two independent length scales in the vertical direction, namely L_{v1} and L_{v2}. SCMC further demonstrated

that the evolution of the integral scales from two simulations of a k^2 spectrum at different rotation rates Ω could be collapsed according to the asymptotic scaling laws

$$L_h \propto B_0^{\frac{1}{5}} t^{\frac{2}{5}} (\Omega t)^{-\frac{1}{5}}, \quad L_{v1} \propto B_0^{\frac{1}{5}} t^{\frac{2}{5}} (\Omega t)^{\frac{3}{5}}, \quad L_{v2} \propto B_0^{\frac{1}{5}} t^{\frac{2}{5}} (\Omega t)^{-\frac{1}{5}}, \tag{10}$$

while for the k^4 spectrum a collapse was achieved using the scaling laws

$$L_h \propto B_2^{\frac{1}{7}} t^{\frac{2}{7}} (\Omega t)^{-\frac{1}{7}}, \quad L_{v1} \propto B_2^{\frac{1}{7}} t^{\frac{2}{7}} (\Omega t)^{\frac{5}{7}}, \quad L_{v2} \propto B_2^{\frac{1}{7}} t^{\frac{2}{7}} (\Omega t)^{-\frac{1}{7}}. \tag{11}$$

3. Asymptotic spectrum similarity

Power-law behavior of both the kinetic energy (Eqs. 5 and 6) and integral length scales (Eqs. 10 and 11) suggest the existence of energy spectra which are asymptotically similar, i.e., the time- and rotation-dependent spectra collapse by appropriately rescaling the wavenumber and spectral density axes. For brevity, we consider here only our results for the k^2 initial conditions. More complete results will be presented in a future publication.

As the first obvious candidate for an asymptotically similar spectrum, we define an axisymmetric energy spectrum as a function of $k_\perp$ and k_3 as

$$\Psi(k_\perp, k_3, t) = \pi k_\perp \langle u_i(\mathbf{k}, t) u_i(\mathbf{k}, t)^* \rangle, \tag{12}$$

where

$$k_\perp = \left(k_1^2 + k_2^2\right)^{\frac{1}{2}} \tag{13}$$

is the horizontal wavenumber perpendicular to the rotation axis, $u_i(\mathbf{k})$ is the Fourier transform of a periodic velocity field $u_i(\mathbf{x})$, * denotes the complex conjugate, and the angular brackets used in (12) denote an average over a horizontal ring in three-dimensional wavespace with center located at a fixed value of k_3. The relationship between the spectrum in (12) and the kinetic energy per unit mass of the fluid is given by

$$\frac{1}{2}\langle \mathbf{u}^2 \rangle = \int_{-\infty}^{\infty} dk_3 \int_0^{\infty} dk_\perp \Psi(k_\perp, k_3, t). \tag{14}$$

An attempt to construct a similarity form directly for the spectrum $\Psi(k_\perp, k_3, t)$ is impeded by the existence of two distinct vertical integral scales in the rotating flow. The choice of an appropriate length scale for rescaling k_3 is thus ambiguous, making it unlikely that the full spectrum $\Psi(k_\perp, k_3, t)$ will be asymptotically similar. We may, however, integrate out the vertical wavenumber from the spectrum defined in (12) to construct an energy spectrum which is a function only of the horizontal wavenumber:

$$\Psi_\perp(k_\perp, t) = \int_{-\infty}^{\infty} dk_3 \Psi(k_\perp, k_3, t). \tag{15}$$

The simulation results have shown that there is only a single horizontal length scale (10) which may be used to scale the horizontal wavenumber $k_\perp$. This allows us to propose the following general form for the similarity state of the spectrum $\Psi_\perp$:

$$\Psi_\perp(k_\perp, t) = \langle \mathbf{u}^2 \rangle L_h \widehat{\Psi}_\perp(L_h k_\perp). \tag{16}$$

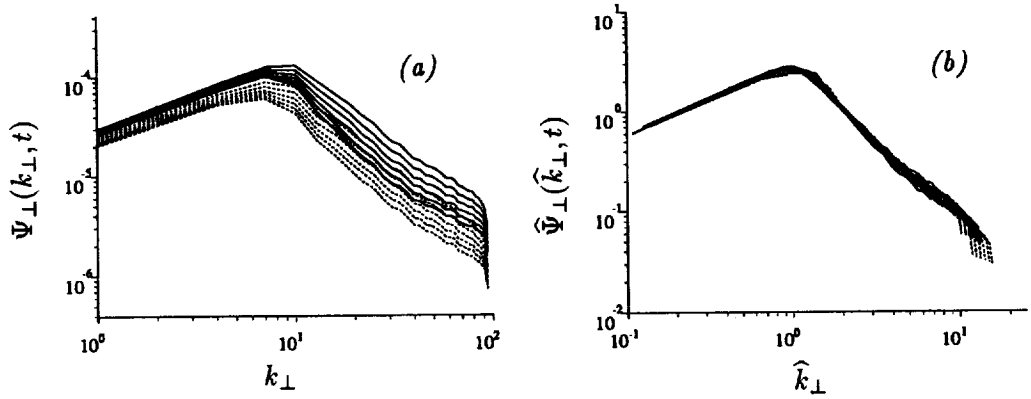

FIGURE 3. Time development of $\Psi_\perp(k_\perp)$. ---- $\Omega = 0.5$; —— $\Omega = 1.0$. (*a*) unscaled; (*b*) scaled.

Making use of the known asymptotic behavior of the kinetic energy (5) and integral scales (10), the similarity state (16) is given explicitly as

$$\Psi_\perp(k_\perp,t) = B_0^{\frac{3}{5}} t^{-\frac{4}{5}} (\Omega t)^{\frac{2}{5}} \widehat{\Psi}_\perp(\widehat{k}_\perp), \qquad \widehat{k}_\perp = B_0^{\frac{1}{5}} t^{\frac{2}{5}} (\Omega t)^{-\frac{1}{5}} k_\perp . \tag{17}$$

Shown in Fig. 3 are the unscaled and scaled spectra $\Psi_\perp(k_\perp,t)$ and $\widehat{\Psi}_\perp(\widehat{k}_\perp,t)$ after the flows have evolved sufficiently to be considered asymptotic in the sense that rotation effects are important (low Rossby numbers) and the statistics follow power-law forms. Spectra from calculations using both non-zero rotation rates have been included in the figures. While the decay with increasing time and the dependence on rotation rate is evident in Fig. 3*a*, the scaled spectra and wavenumbers (17) in Fig. 3*b* show a remarkable collapse, indicating that $\widehat{\Psi}_\perp$ is independent of both time and rotation rate. The results shown in Fig. 3*b* thus confirm the similarity state given by (17). This is a significant result since we have succeeded in reducing the number of independent variables in the problem from four, ($k_\perp$, t, Ω, and B_0), where B_0 represents the effect of initial conditions, to simply one, ($\widehat{k}_\perp$).

We must still confront the difficulty of finding similarity spectra which are functions of the vertical wavenumber k_3. We know from the LES results that two vertical length scales exist, one associated with the horizontal velocities and the other with the vertical velocities. This suggests splitting the energy spectrum into two spectra, each separately related to the horizontal or vertical velocities. A simple splitting, however, does not take into account the constraint imposed by the continuity equation on the flow field. Rather, we proceed to define spectra (Herring 1974) by first projecting the Fourier components of the velocity field onto two unit vectors perpendicular to $\mathbf{k}$ (the velocity component parallel to $\mathbf{k}$ is zero by virtue of the continuity equation):

$$u_i(\mathbf{k}) = \phi_1(\mathbf{k}) e_i^{(1)}(\mathbf{k}) + \phi_2(\mathbf{k}) e_i^{(2)}(\mathbf{k}), \tag{18}$$

where

$$\mathbf{e}^{(1)}(\mathbf{k}) = \frac{\mathbf{k} \times \mathbf{\Omega}}{|\mathbf{k} \times \mathbf{\Omega}|}, \quad \mathbf{e}^{(2)}(\mathbf{k}) = \frac{\mathbf{k} \times \mathbf{e}^{(1)}(\mathbf{k})}{|\mathbf{k} \times \mathbf{e}^{(1)}(\mathbf{k})|}. \tag{19}$$

We note that the field $\phi_1(\mathbf{k})$ consists only of horizontal velocity fluctuations, whereas the field $\phi_2(\mathbf{k})$ contains both horizontal and vertical fluctuations. We then use the scalar fields $\phi_1(\mathbf{k})$ and $\phi_2(\mathbf{k})$ to define energy spectra in analogy to (12):

$$\Psi^{(1)}(k_\perp, k_3, t) = \pi k_\perp \langle \phi_1(\mathbf{k}, t) \phi_1(\mathbf{k}, t)^* \rangle, \tag{20}$$

$$\Psi^{(2)}(k_\perp, k_3, t) = \pi k_\perp \langle \phi_2(\mathbf{k}, t) \phi_2(\mathbf{k}, t)^* \rangle, \tag{21}$$

where we have now separated the energy spectrum into two spectra:

$$\Psi(k_\perp, k_3, t) = \Psi^{(1)}(k_\perp, k_3, t) + \Psi^{(2)}(k_\perp, k_3, t). \tag{22}$$

The significance of this separation can be seen by expressing the integral length scales L_{v1} and L_{v2} of (9) in terms of $\Psi^{(1)}$ and $\Psi^{(2)}$, i.e.,

$$L_{v1} = \frac{\pi}{\langle u_1^2 + u_2^2 \rangle} \int_0^\infty dk_\perp \Psi^{(1)}(k_\perp, 0), \tag{23}$$

and

$$L_{v2} = \frac{\pi}{\langle u_3^2 \rangle} \int_0^\infty dk_\perp \Psi^{(2)}(k_\perp, 0). \tag{24}$$

The LES results show that the horizontal and vertical mean-square velocity fluctuations decay asymptotically with the same power-law form, so that (23) and (24) serve the hopeful purpose of matching the two independent vertical integral scales to the two different spectra.

In analogy to the similarity form given in (16), we now postulate the following general similarity states of the form

$$\Psi^{(1)}(k_\perp, k_3, t) = \langle \phi_1^2 \rangle l_1^h l_1^v \widehat{\Psi}^{(1)}(l_1^h k_\perp, l_1^v k_3), \tag{25a}$$

$$\Psi^{(2)}(k_\perp, k_3, t) = \langle \phi_2^2 \rangle l_2^h l_2^v \widehat{\Psi}^{(2)}(l_2^h k_\perp, l_2^v k_3), \tag{25b}$$

where $\langle \phi_1^2 \rangle$, l_1^h, l_1^v, and $\langle \phi_2^2 \rangle$, l_2^h, l_2^v are the mean-square fluctuations and horizontal and vertical integral scales associated with the $\Psi^{(1)}$ and $\Psi^{(2)}$ spectra, respectively. The relations between the mean-square fluctuations, the integral scales, and the spectra are given for reference by

$$\langle \phi_{1,2}^2 \rangle = \int_{-\infty}^\infty dk_3 \int_0^\infty dk_\perp \Psi^{(1,2)}(k_\perp, k_3, t), \tag{26}$$

and

$$l_{1,2}^v = \frac{\pi}{\langle \phi_{1,2}^2 \rangle} \int_0^\infty dk_\perp \Psi^{(1,2)}(k_\perp, 0, t), \quad l_{1,2}^h = \frac{1}{\langle \phi_{1,2}^2 \rangle} \int_{-\infty}^\infty dk_3 \int_0^\infty \frac{\Psi^{(1,2)}(k_\perp, k_3, t)}{k_\perp}. \tag{27}$$

We have computed the amplitudes and integral scales given by (26) and (27) from the LES database. The mean-square values $\langle\phi_1^2\rangle$ and $\langle\phi_2^2\rangle$ decay asymptotically at the same rate as the total kinetic energy per unit mass as given in (5), and the horizontal integral scales l_1^h and l_2^h and vertical integral scales l_1^v and l_2^v grow asymptotically as L_h (for both horizontal integral scales) and L_{v1} and L_{v2}, respectively, as given by (10).

Although the similarity states proposed in (25) appear to be reasonable, a closer examination reveals a further problem. We recall that the asymptotic form of the energy and integral scales were constructed on the basis of the invariant B_0, related to the form of the energy spectrum near zero wavenumber. Assuming a flow field starting from isotropic initial conditions (as in our simulations), the forms of the spectra $\Psi^{(1)}(k_\perp, k_3, t)$ and $\Psi^{(2)}(k_\perp, k_3, t)$ near $k = 0$ are

$$\begin{aligned}\Psi^{(1)}(k_\perp, k_3, t) &= 2\pi k_\perp (B_0 + O(k)),\\ \Psi^{(2)}(k_\perp, k_3, t) &= 2\pi k_\perp (B_0 + O(k)),\end{aligned} \tag{28}$$

where $O(k)$ represents terms which vanish as $k = \left(k_\perp^2 + k_3^2\right)^{1/2} \to 0$ and B_0 is independent of time. Near $k = 0$ the similarity forms of the spectra must necessarily be

$$\widehat{\Phi}^{(1)}(l_1^h k_\perp, l_1^v k_z) \sim 2\pi l_1^h k_\perp, \qquad \widehat{\Phi}^{(2)}(l_2^h k_\perp, l_2^v k_z) \sim 2\pi l_2^h k_\perp; \tag{29}$$

and substituting (28) and (29) into (25) yields

$$B_0 \propto \langle\phi_1^2\rangle (l_1^h)^2 l_1^v, \qquad B_0 \propto \langle\phi_2^2\rangle (l_2^h)^2 l_2^v. \tag{30}$$

Eq. (30) is an important result in that it provides two additional constraints on the allowed form of an asymptotic similarity state based on the invariant B_0. The second constraint of (30) can be seen to be satisfied by the LES results, where

$$\langle\phi_2^2\rangle \propto B_0^{\frac{2}{5}} t^{-\frac{6}{5}} (\Omega t)^{\frac{3}{5}}, \quad l_2^h \propto B_0^{\frac{1}{5}} t^{\frac{2}{5}} (\Omega t)^{-\frac{1}{5}}, \quad l_2^v \propto B_0^{\frac{1}{5}} t^{\frac{2}{5}} (\Omega t)^{-\frac{1}{5}}. \tag{31}$$

However, the first constraint of (30) is widely violated by the LES results due to the rapid growth in the vertical integral scale:

$$\langle\phi_1^2\rangle \propto B_0^{\frac{2}{5}} t^{-\frac{6}{5}} (\Omega t)^{\frac{3}{5}}, \quad l_1^h \propto B_0^{\frac{1}{5}} t^{\frac{2}{5}} (\Omega t)^{-\frac{1}{5}}, \quad l_2^v \propto B_0^{\frac{1}{5}} t^{\frac{2}{5}} (\Omega t)^{\frac{3}{5}}, , \tag{32}$$

so that

$$\langle\phi_1^2\rangle (l_1^h)^2 l_1^v \propto B_0 (\Omega t)^{\frac{4}{5}}.$$

The similarity state in (25a) constructed for $\Phi^{(1)}(k_\perp, k_3, t)$ must thus be in error. However, the similarity state in (25b) constructed for $\Phi^{(2)}(k_\perp, k_3, t)$ may possibly be correct in so far as the constraint given by the second of (30) is satisfied.

To test the correctness of the similarity state for $\Phi^{(2)}(k_\perp, k_3, t)$, we isolate the troublesome k_3 dependence of the spectrum by integrating over $k_\perp$ to obtain the (usual) one-dimensional spectrum

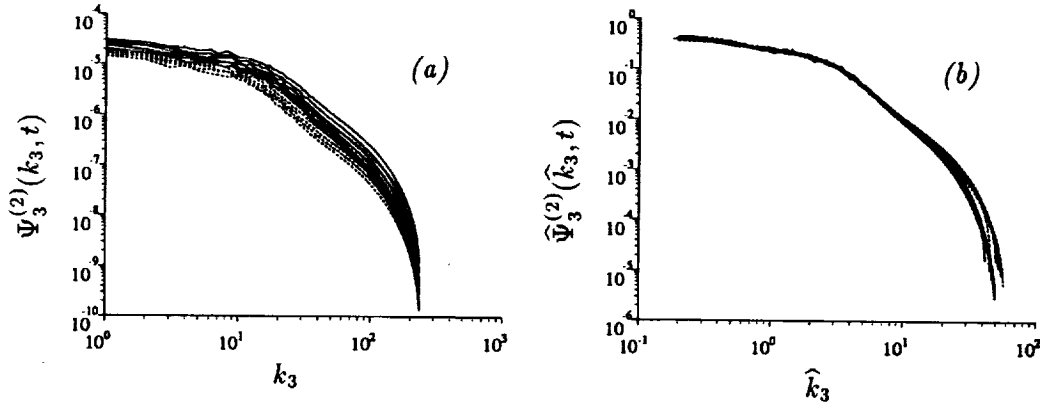

FIGURE 4. Time development of $\Psi_3^{(2)}(k_3)$. ---- $\Omega = 0.5$; —— $\Omega = 1.0$. (*a*) unscaled; (*b*) scaled.

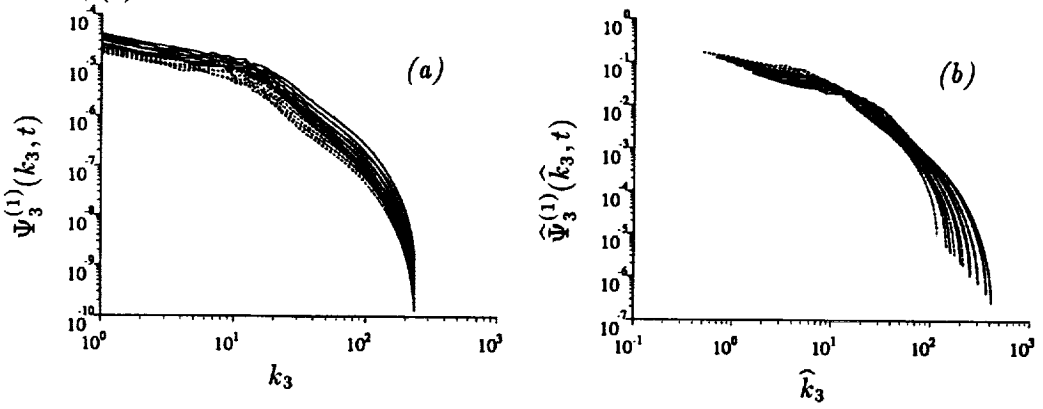

FIGURE 5. Time development of $\Psi_3^{(1)}(k_3)$. ---- $\Omega = 0.5$; —— $\Omega = 1.0$. (*a*) unscaled; (*b*) scaled.

$$\Psi_3^{(2)}(k_3,t) = \int_0^\infty dk_\perp \Psi^{(2)}(k_\perp,k_3,t)\,; \tag{33}$$

and the corresponding similarity state is postulated to be

$$\Psi_3^{(2)}(k_3,t) = \langle\phi_2^2\rangle l_2^v \widehat{\Psi}_\perp(l_2^v k_3)\,, \tag{34}$$

which using (31), may be written explicitly as

$$\Psi_3^{(2)}(k_3,t) = B_0^{\frac{3}{5}} t^{-\frac{4}{5}} (\Omega t)^{\frac{2}{5}} \widehat{\Psi}_3^{(2)}(\widehat{k}_3)\,, \qquad \widehat{k}_3 = B_0^{\frac{1}{5}} t^{\frac{2}{5}} (\Omega t)^{-\frac{1}{5}} k_3\,. \tag{35}$$

Shown in Fig. 4 are the unscaled spectra $\Psi_3^{(2)}(k_3,t)$ and the scaled spectra $\widehat{\Psi}_3^{(2)}(\widehat{k}_3,t)$ obtained from (35). As before, results for both non-zero rotation rates are shown in the figure. In Fig. 4*a* the spectra at different times and rotation rates

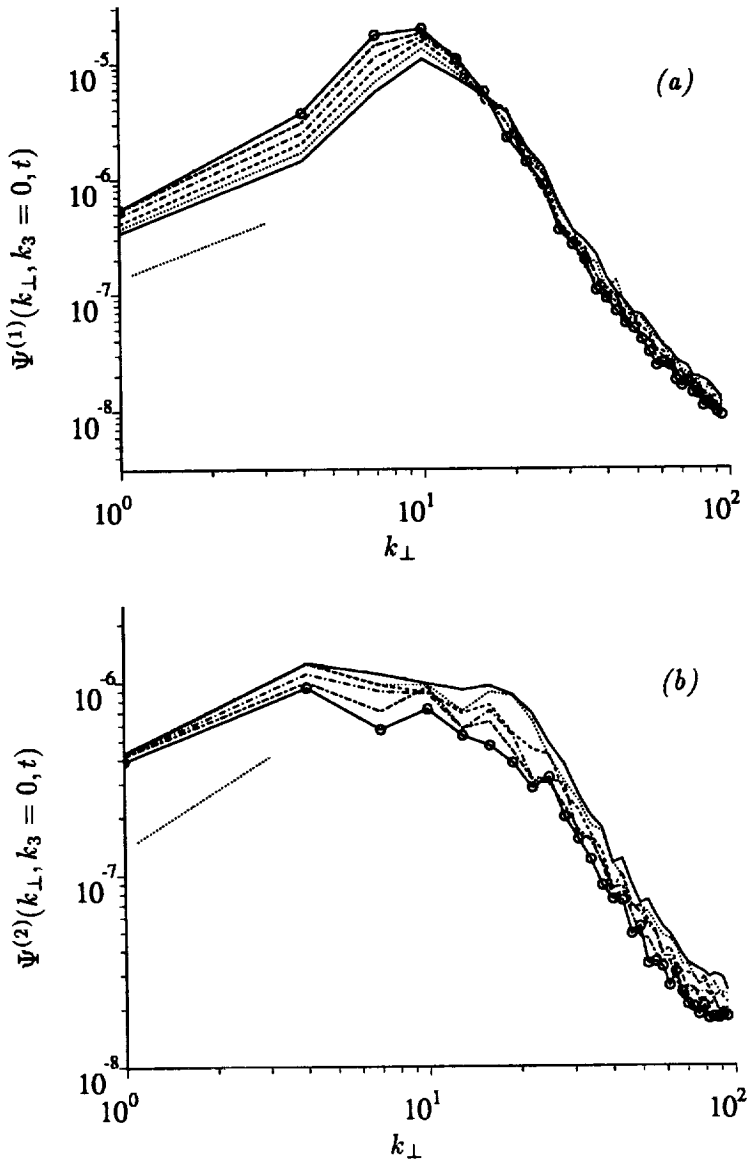

FIGURE 6. Time development of $\Psi^{(1)}(k_\perp, k_3)$ (Fig. 6a) and $\Psi^{(2)}(k_\perp, k_3)$ (Fig 6b) for $k_3 = 0$ and $\Omega = 1.0$. Increasing time is from —— to o——o ; ····· asymptotic behavior as $k_\perp \to 0$ (Eqn. 29).

are clearly distinguishable whereas in Fig. 4*b* the spectra $\widehat{\Psi}_3^{(2)}(\widehat{k}_3, t)$ for the times plotted and both Ω collapse onto a single curve. Together with the previous results of Fig. 3, we have thus confirmed the complete similarity state of $\Psi^{(2)}(k_\perp, k_3, t)$ given by (25b).

For comparison, the troublesome one-dimensional spectrum $\Psi^{(1)}(k_3, t)$ and the

scaled spectrum corresponding to the assumed similarity form given by (25a) are shown in Fig. 5. As anticipated from the inconsistency of the assumed similarity form with the constraint given by the first of (30), the rescaling shown in Fig. 5*b* does not collapse $\widehat{\Psi}_3^{(1)}(\widehat{k}_3)$ onto a single curve.

Thus we have demonstrated spectral similarity for three out of four spectra, namely $\Psi_\perp^{(1)}(k_\perp, t)$, $\Psi_\perp^{(2)}(k_\perp, t)$, and $\Psi_3^{(2)}(k_3, t)$ are asymptotically similar, whereas $\Psi_3^{(1)}(k_3, t)$ is decidedly not.

Further evidence of the anomalous asymptotic behavior of $\Psi_3^{(1)}$ is provided in Fig. 6. Shown in the figure, for $\Omega = 1.0$, are $\Psi^{(1)}$ (Fig. 6*a*) and $\Psi^{(2)}$ (Fig. 6*b*) as a function of $k_\perp$ for $k_3 = 0$. From (28), the spectra in these figures should follow the asymptotic form $\Psi^{(1,2)}(k_\perp, k_3 = 0, t) \sim 2\pi k_\perp B_0$ as $k_\perp \to 0$. Considering Fig. 6*b*, $\Psi^{(2)}(k_\perp, 0, t)$ decays as one would expect from a decaying three-dimensional turbulence. The energy at larger values of $k_\perp$ decay more rapidly than the energy at smaller values, and consequently the peak of the spectrum systematically moves to lower wavenumbers. The invariance of the form of the spectrum as $k_\perp \to 0$ is respected. The spectrum $\Psi^{(1)}(k_\perp, 0, t)$ shown in Fig. 6*a*, however, behaves much differently. A strong increase in the energy at small values of $k_\perp$ is clearly evident. The invariance of the spectrum as $k_\perp \to 0$ is a rigorous result, yet appears to be irrelevant to the time-development of this spectrum. It is important to note that the spectrum $\Psi^{(1)}(k_\perp, 0, t)$ corresponds to two-dimensional, two-component motions, and what we are observing in Fig. 6*a* is apparently a reverse cascade of energy from small to large scales, well-known within the context of two-dimensional turbulence. The existence of a reverse cascade may be the reason why a similarity state based on the invariance of the low wavenumber coefficient does not develop for the $\Psi^{(1)}$ spectrum. The establishment of a two-dimensional reverse cascade is an important feature of three-dimensional turbulence in a rotating frame, and obviously requires a deeper understanding than we have achieved thus far. Other recent investigations (Bartello *et al.* 1994; Hossain 1994) have also confronted this very question, although from a different perspective than the present work.

Finally, the strong reverse cascade of energy of the two-dimensional, two-component motions has interesting implications as to the asymptotic structural evolution of rotating homogeneous turbulence. The reader is referred to Cambon, Mansour & Squires (1994) (contained in this proceedings) for further discussion of these issues.

Acknowledgments

The authors are grateful to Dr. R. Rogallo and Dr. A. Wray for their assistance with the VECTORAL compiler and homogeneous turbulence code used during the course of this study. Helpful discussions with C. Cambon, A. Mahalov, and W. C. Reynolds are also appreciated. K. D. S. was partially supported for this work by the American Society of Engineering Education.

REFERENCES

AUPOIX, B. 1984 Eddy viscosity subgrid-scale models for homogeneous turbulence. *Proc. of Macroscopic Mod. Turb. Flows, Lecture Notes in Phys.* **230**, 45.

BARTELLO, P., MÉTAIS, O. & LESIEUR, M. 1994 Coherent structures in rotating three-dimensional turbulence. *J. Fluid Mech.* **273,** 1.

CAMBON, C. & JACQUIN, L. 1989 Spectral approach to non-isotropic turbulence subjected to rotation. *J. Fluid Mech.* **202,** 295–317.

CAMBON, C., MANSOUR, N. N. & SQUIRES, K. D. 1994 Anisotropic structure of homogeneous turbulence subjected to uniform rotation. *Proc. of the 1994 Summer Program,* NASA/Stanford Center for Turbulence Research.

CHOLLET, J. P. & LESIEUR, M. 1981 Parameterization of small scales of three-dimensional isotropic turbulence utilizing spectra closures. *J. Atmos. Sci.* **38,** 2747.

CHASNOV, J. R. 1994 Similarity states of passive scalar transport in isotropic turbulence. *Phys. Fluids.* **6,** 1036.

HERRING, J. R. 1974 Approach of axisymmetric turbulence to isotropy. *Phys. Fluids.* **17,** 859.

HOSSAIN, M. 1994 Reduction in the dimensionality of turbulence due to a strong rotation. *Phys. Fluids A.* **6,** 1077.

KRAICHNAN, R. H. 1976 Eddy viscosity in two and three dimensions. *J. Atmos. Sci.* **33,** 1521.

ROGALLO, R. S. 1981 Numerical experiments in homogeneous turbulence. *NASA TM 81315.*

SQUIRES, K. D., CHASNOV, J. R., MANSOUR, N. N. & CAMBON, C. 1993 Investigation of the asymptotic state of rotating turbulence using large-eddy simulation. *Annual Research Briefs,* NASA/Stanford Center for Turbulence Research, 157-170.

SQUIRES, K. D., CHASNOV, J. R., MANSOUR, N. N. & CAMBON, C. 1994 The asymptotic state of rotating homogeneous turbulence at high Reynolds number. *AGARD Conf. Proc. CP-551,* in press.